Bioorganic Chemistry 92 (2019) 103261

Contents lists available at ScienceDirect

Bioorganic Chemistry

journal homepage: www.elsevier.com/locate/bioorg

Optimization study towards more potent thiazolidine-2,4-dione IKK-β modulator: Synthesis, biological evaluation and *in silico* docking simulation

Ahmed Elkamhawy[a,b,*,1], Nam youn Kim[a,1], Ahmed H.E. Hassan[c], Jung-eun Park[a], Jeong-Eun Yang[a], Mohamed H. Elsherbeny[a,d], Sora Paik[a], Kwang-Seok Oh[e], Byung Ho Lee[e], Mi Young Lee[e], Kye Jung Shin[f], Ae Nim Pae[d,g], Kyung-Tae Lee[h], Eun Joo Roh[a,d,*]

[a] Chemical Kinomics Research Center, Korea Institute of Science and Technology (KIST), Seoul 02792, Republic of Korea
[b] Department of Pharmaceutical Organic Chemistry, Faculty of Pharmacy, Mansoura University, Mansoura 35516, Egypt
[c] Department of Medicinal Chemistry, Faculty of Pharmacy, Mansoura University, Mansoura 35516, Egypt
[d] Division of Bio-Medical Science & Technology, KIST School, Korea University of Science and Technology, Seoul 02792, Republic of Korea
[e] Therapeutics & Biotechnology Division, Korea Research Institute of Chemical Technology, 141 Gajeong-ro, Yuseong, Daejeon 34114, Republic of Korea
[f] Integrated Research Institute of Pharmaceutical Sciences, College of Pharmacy, The Catholic University of Korea, Bucheon-si, Gyeonggi-do 14662, Republic of Korea
[g] Convergence Research Center for Diagnosis, Treatment and Care System of Dementia, Korea Institute of Science and Technology (KIST), Seoul 02792, Republic of Korea
[h] Department of Life and Nanopharmaceutical Sciences, Kyung Hee University, Seoul 02447, Republic of Korea

ARTICLE INFO

Keywords:
IKK-β modulator
NF-κB signaling pathway
Thiazolidine-2,4-dione
Molecular docking

ABSTRACT

Inhibition of IKK-β (inhibitor of nuclear factor kappa-B kinase subunit beta) has been broadly documented as a promising approach for treatment of acute and chronic inflammatory diseases, cancer, and autoimmune diseases. Recently, we have identified a novel class of thiazolidine-2,4-diones as structurally novel modulators for IKK-β. Herein, we report a hit optimization study *via* analog synthesis strategy aiming to acquire more potent derivative(s), probe the structure activity relationship (SAR), and get reasonable explanations for the elicited IKK-β inhibitory activities though an *in silico* docking simulation study. Accordingly, a new series of eighteen thiazolidine-2,4-dione derivatives was rationally designed, synthesized, identified with different spectroscopic techniques and biologically evaluated as noteworthy IKK-β potential modulators. Successfully, new IKK-β potent modulators were obtained, including the most potent analog up-to-date **7m** with IC_{50} value of 260 nM. A detailed structure activity relationship (SAR) was discussed and a mechanistic study for **7m** was carried out indicating its irreversible inhibition mode with IKK-β (K_{inact} value = 0.01 (min^{-1})). Furthermore, the conducted *in silico* simulation study provided new insights for the binding modes of this novel class of modulators with IKK-β.

1. Introduction

In view of the fact that most research efforts have focused on modulation of the ATP binding pocket which bears similarities across various kinases, development of a selective kinase inhibitor is not easily achievable. Such poorly selective ATP competitive small molecules could face limited clinical applications [1]. As a result, allosteric kinase modulators have recently gained more attraction in the field as targeting the more variable sites of kinases offers better opportunities to afford more efficient and selective inhibitors [2–4]. In addition, covalent modulators characterized by their irreversible binding mode could be more effective than the classical reversible inhibitors, yet, are devoid from the previously doubted toxicities [5–10]. Lately, the concept of covalent inhibition has been extended to the development of covalent allosteric inhibitors possessing higher levels of selectivity as well as potency [11–13].

The transcription factor "nuclear factor kappa-light-chain-enhancer of activated B cells" (NF-κB) elevates the expression of more than 500 genes including various pro-inflammatory genes [14–17]. Additionally, NF-κB-triggered genes expression invokes immunological responses, cells' proliferation, as well as apoptosis [18,19]. The canonical NF-κB signaling pathway is activated by IKK-β kinase (Inhibitor of nuclear factor kappa-B kinase subunit beta) which phosphorylates IκB (inhibitor of NF-κB) resulting in release and translocation of NF-κB into the nucleus [20]. Accordingly, inhibition of IKK-β might be a successful strategy for treatment of acute and chronic inflammatory diseases,

* Corresponding authors at: Chemical Kinomics Research Center, Korea Institute of Science and Technology (KIST), Seoul 02792, Republic of Korea.
E-mail addresses: a_elkamhawy@mans.edu.eg, a.elkamhawy@kist.re.kr (A. Elkamhawy), r8636@kist.re.kr (E.J. Roh).
[1] Both authors contributed equally to this work.

https://doi.org/10.1016/j.bioorg.2019.103261
Received 23 December 2018; Received in revised form 3 September 2019; Accepted 5 September 2019
Available online 07 September 2019

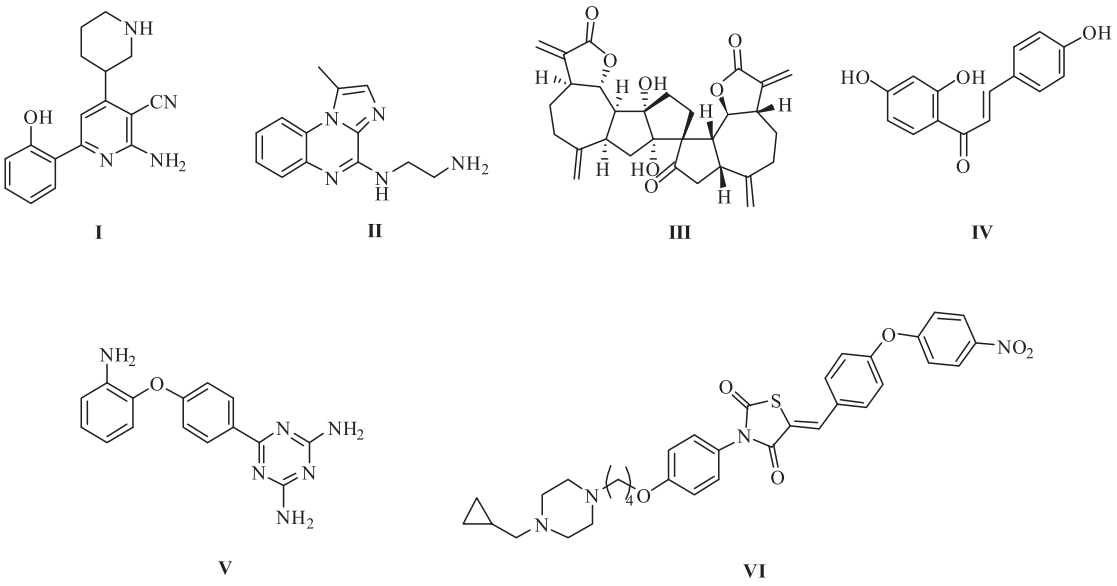

Fig. 1. IKK-β inhibitory small molecules in literature.

cancer, and autoimmune diseases [20–24].

However diverse chemical scaffolds have been reported in literature for the development of NF-κB signaling pathway modulators including IKK-β inhibitors [18,23], to the best of our knowledge, most of the developed IKK-β targeting agents have a reversible competitive inhibition mode of action; for example, Bayer Pharmaceuticals' compound (**I**, Fig. 1) [25]. Despite the advantages of the irreversible allosteric modulators over the reversible classical ATP competitive inhibitors as mentioned previously, even reversible allosteric IKK-β inhibitors have been found in literature scarcely (e.g. BMS-345541 (**II**); a non-selective allosteric inhibitor of both IKK-α and IKK-β [16]). Accordingly, there is still a vigorous need to find novel small molecules as covalent allosteric inhibitors targeting IKK-β kinase.

A recent study showed the natural product (+)-ainsliadimer (**III**) to covalently inhibit IKK-β at an allosteric site [26]. In another article, covalent binding of the natural product isoliquiritigenin (**IV**) was also found to reduce the activity of T Lymphocytes [27]. Recently, 1,3,5-triazine-2,4-diamine derivative (**V**) has been reported as an IKK-β inhibitor and used as a starting point to develop orthosteric IKK-β inhibitors [28]. In the same study, a 2-imino-4-thiazolidin-4-one derivative was found as a hit IKK-β modulator possessing high IC_{50} value of 97.4 μM. In our recent research, we have developed the latter hit compound into novel thiazolidine-2,4-dione derivatives which showed a promising *in vitro* inhibitory activity over IKK-β kinase *via* covalent allosteric mechanism of action [29]. As shown in Fig. 2, one of our reported derivatives (**VI**), with IKK-β IC_{50} value of 1.5 μM, possessed a butyl chain linker bridging the piperazinyl moiety to the *para* position of the phenyl ring which is attached to the nitrogen atom of the thiazolidine-2,4-dione scaffold. In our previous report, the terminal *N*-substituent on the piperazine ring had a crucial effect on the elicited inhibitory activity; for example, *N*-cyclopropylmethyl moiety exerted higher activity than *N*-substituents possessing the more polar oxygen or sulfur atom. In view of that, in this report, we aimed at hit optimization through diverse structural modifications over the lead compound **VI** as a trial to acquire more potent analog(s), probe the structure activity correlation, and to understand the reasons underlying behind the different binding modes of this novel class of modulators with IKK-β.

Our design approach focused on switching the terminal *N*-substituent to methyl in order to explore the effect of the one carbon substituent that might result in extending the molecule in attempts to block the solvent access to Trp58 residue of IKK-β. In addition, *N*-methylpiperazine moiety may allow better interaction of the molecule with the solvent at this area. Furthermore, since the structure of IKK-β incorporates an important cysteine residue (Cys46) which exists in the vicinity of an allosteric site located close to the catalytic ATP pocket (protein databank code: 3QA8) [30], the observed irreversible allosteric inhibition might result from Michael addition of thiol group to the double bond of benzylidene moiety of compound **VI**. Also, since variable substituents attached to the benzylidene moiety might exert different electron push-pull, which would affect the Michael addition of thiol group of cysteine, we have designed a new thiazolidine-2,4-dione-based series possessing variable fused as well as unfused cycles characterized with different electron densities to allow enhancing and fine tuning the elicited covalent inhibition (Fig. 2).

2. Results and discussion

2.1. Chemistry

As presented in Scheme 1, synthesis of the final compounds (**7a–r**) was achieved starting from the commercially available starting material 4-aminophenol (**1**) *via* amide coupling reaction with chloroacetyl chloride to yield 2-chloro-*N*-(4-hydroxyphenyl)acetamide (**2**). The chloro group in compound **2** has been substituted with thiocyanate followed by cyclization to afford 3-(4-hydroxyphenyl)-2-iminothiazolidin-4-one **3** [31]. Acidic hydrolysis of compound **3** using 2% HCl aqueous solution gave the thiazolidine-2,4-dione intermediate **4** [32]. *O*-Alkylation of the phenolic OH with 1,4-diiodobutane provided derivative **5** possessing the butyl chain linker. *N*-Alkylation of 1-methylpiperazine with the prepared derivative **5** gave the corresponding thiazolidine-2,4-dione derivative **6**. Finally, Knoevenagel condensation reaction has been used to react various aldehyde derivatives with intermediate **6** in order to afford the target compounds (**7a–r**) [33].

2.2. Biological evaluation

2.2.1. In vitro IKK-β induced phosphorylation modulation

The target compounds **7a–r** were evaluated for their potential *in vitro* IKK-β inhibitory activity employing 5-FAM (5-carboxyfluorescein) labeled IκBα-derived polypeptide (5-FAMGRHDSGLDSMK-NH_2; R7574, MDS Analytical Technologies) as a substrate for IKK-β in an IMAP® based fluorescence assay [34]. As indicated in Table 1, although introducing the isosteric 5-(2,3-dihydrobenzofuranyl) moiety on the exomethylene group afforded an inactive compound **7a**, compound **7b**

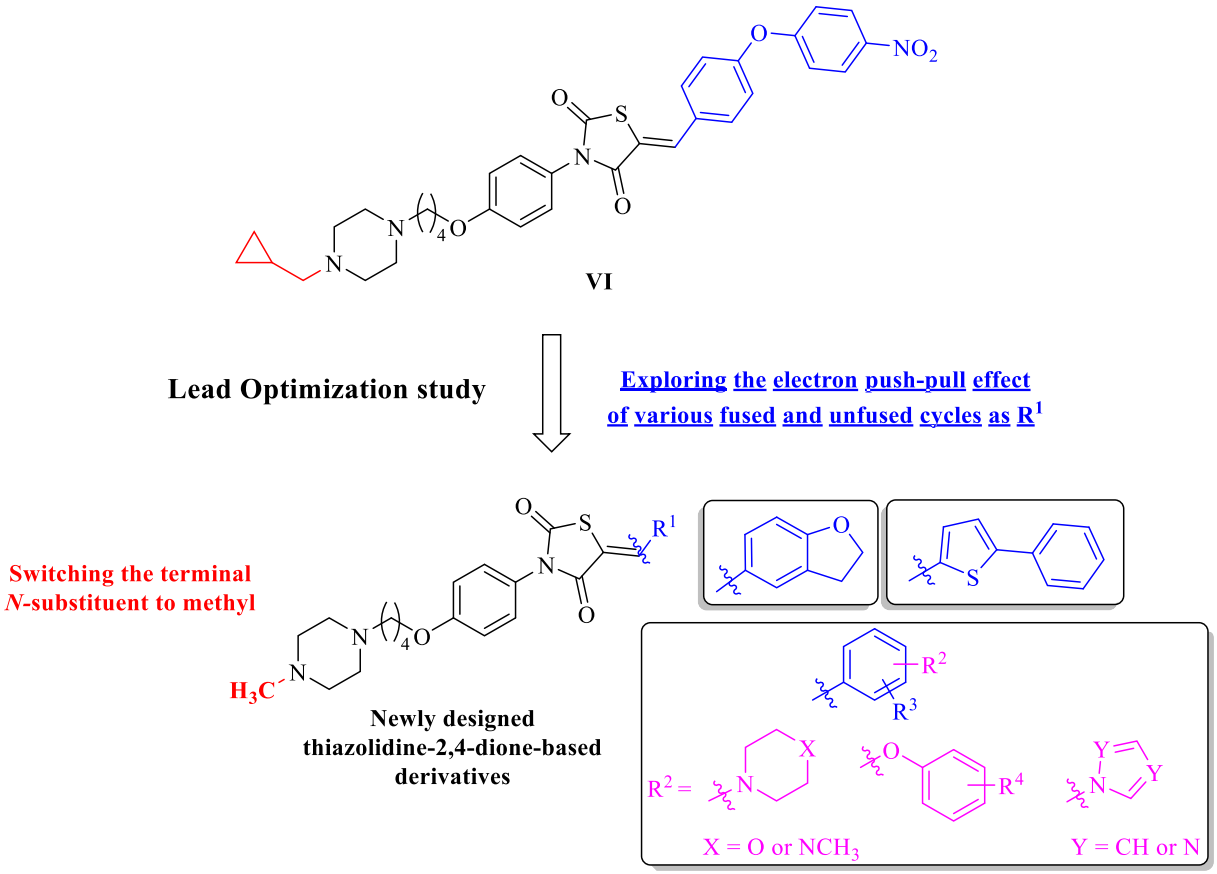

Fig. 2. Lead optimization design of compound **VI** towards new thiazolidine-2,4-dione derivatives.

with the aromatic 2-(5-phenylthienyl) group was significantly active eliciting 74.1% inhibition at 10 μM single dose concentration with measured IC_{50} equals to 2.52 μM. The significant improvement of analog **7b** activity might indicate that a suitable unfused aromatic moiety attached to the exomethylene carbon is required to obtain an active IKK-β inhibitor.

Accordingly, the rest of designed analogs were prepared incorporating variably substituted phenyl rings on the exomethylene group. Five compounds (**7c**, **7d**, **7e**, **7f** and **7g**) possessing the five membered nitrogen containing heterocycles 1*H*-pyrazole, 1*H*-imidazole and 1*H*-1,2,4-triazole as substituents on the phenyl ring were synthesized and evaluated. While compound **7g** having 1*H*-imidazol-1-yl substituent at *meta* position did not elicit significant activity, compounds **7c**, **7d**, **7e** and **7f** having the heterocyclic ring substituents at *para* position elicited low micromolar IC_{50} values. This might be due to intolerance of the binding site to the steric requirements of the introduced heterocyclic ring as a substituent at the *meta* position, meanwhile, it is tolerated in case of *para* position. However, the less

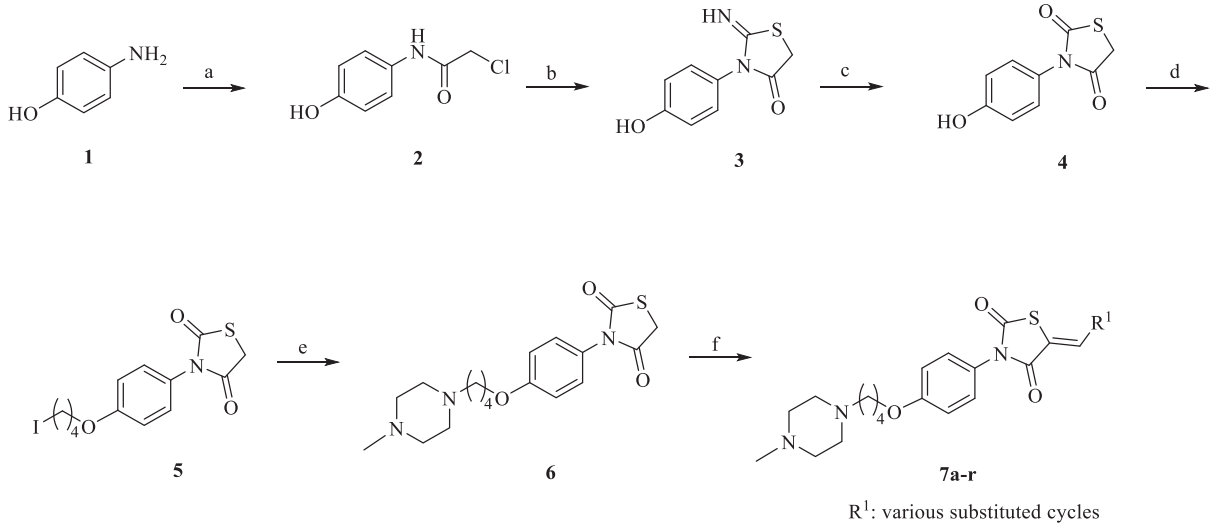

Scheme 1. Reagents and reaction conditions: (a) chloroacetyl chloride, DCM, 0 °C, 1.5 h, rt, 3 h; (b) KSCN, acetone, 65 °C, 7 h; (c) 2% HCl aqueous solution, 100 °C, 7 h; (d) 1,4-diiodobutane, K_2CO_3, MeCN, 95 °C, 7 h; (e) 1-methylpiperazine, K_2CO_3, MeCN, rt, 9 h; (f) appropriate aldehyde derivative, NaOAc, AcOH, 110 °C, 16 h.

Table 1
Results of IKK-β assay for the newly synthesized target compound **7**.

Cpd	R^1	IKK-β assay		Cpd	R^1	IKK-β assay	
		% Inhibition[a]	IC_{50} (μM)[b]			% Inhibition[a]	IC_{50} (μM)[b]
7a		0.8	—	**7j**	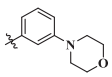	0.1	—
7b	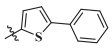	74.1	2.52 ± 0.20	**7k**	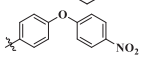	71.3	0.39 ± 0.01
7c	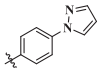	82.5	3.81 ± 0.16	**7l**	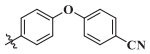	67.7	0.63 ± 0.03
7d	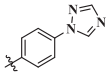	77.3	4.33 ± 0.49	**7m**	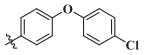	63.8	0.26 ± 0.02
7e	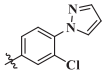	82.2	3.96 ± 0.19	**7n**	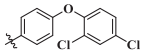	76.7	0.81 ± 0.08
7f	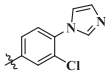	67.6	7.79 ± 0.28	**7o**	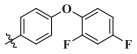	68.4	0.85 ± 0.09
7g	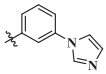	5.8	—	**7p**	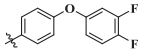	77.9	2.34 ± 0.10
7h	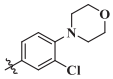	85.9	1.20 ± 0.28	**7q**	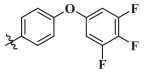	72.4	0.85 ± 0.10
7i	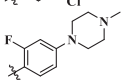	48.4	—	**7r**	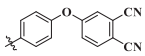	89.0	1.02 ± 0.13

[a] Percent inhibition at single dose concentration of 10 μM.
[b] IC_{50} values (μM) exhibited by the final compounds **7a–r**, and expressed as means ± S.D.

steric demand of the smaller chloro substituents results in the active compounds **7e** and **7f** having *m*eta chloro substituent, as well as, 1*H*-pyrazol-1-yl or 1*H*-imidazol-1-yl. Compounds **7c** and **7e** possessing 1*H*-pyrazol-1-yl moiety were more effective and potent than the corresponding compounds **7d** and **7f** having 1*H*-1,2,4-triazol-1-yl or 1*H*-imidazol-1-yl respectively. The results of compounds **7c** and **7e** having the same five membered heterocyclic ring at *para* position reveals a minimal impact on IKK-β inhibitory activity triggered by introduction of a chloro substituent at *meta* position. Replacement of the five membered heterocyclic rings at *para* position of active compounds **7e** and **7f** with an alicyclic amine affords the more potent compound **7 h** with IC_{50} value equals to 1.2 μM. Meanwhile, replacement of the five membered heterocyclic rings at *meta* position of the inactive compound **7 g** resulted also in the inactive compound **7j**. This reinforces the assumption of the limited tolerance of the targeted biological activity to bulky substituents at *meta* position. Also, the results showed that introduction of the electronically amphiphilic fluoro substituent at *ortho* position results in compound **7i** eliciting reduced IKK-β inhibitory activity.

As the IKK-β inhibitory activity tolerates substituents on the *para* position which is quite similar result to our recent finding [29], we explored the effect of various substituted-phenoxy moieties at this position (**7k**, **7l**, **7m**, **7n**, **7o**, **7p**, **7q** and **7r**). Nearly, all of them showed submicromolar IC_{50} values indicating more beneficial impact of substituted-phenoxy moieties over the evaluated five membered heterocyclic rings as well as the alicyclic amines. Compounds possessing the substituents 4-nitrophenoxy and 4-cyanophenoxy (**7k** and **7l**, respectively) with electron withdrawing groups at the 4-position of the phenoxy moiety, as well as, 4-chlorophenoxy (**7m**) having an electronically amphiphilic group at the same position elicited lower IC_{50} values relative to other prepared compounds (0.39, 0.63 and 0.26 μM, respectively). Modification of the phenoxy substituent of compound **7m** by introducing a second chloro group at 2-position afforded the less potent compound **7n**. Replacement of the 2,4-dichloro substituents (**7n**) by the less sterically demanding 2,4-difluoro afforded compound **7o** with almost similar potency. Changing the position of the electronegative fluoro groups to the 3,4-position resulted in less potent compound **7p**. However, compound **7q** with the 3,4,5-trifluorophenoxy moiety showed similar potency to that of analog **7o**.

2.2.2. Mechanistic study of the induced IKK-β inhibition

Compound **7m**, the most active inhibitor in the newly synthesized series with IC_{50} value of 260 nM over the IKK-β, was further investigated for its elicited inhibition mode; the kinetic dose-response curves (measurement intervals equivalent to 0, 20, 40 and 60 min) were generated using approximately three-fold dilutions (30, 10, 3, 1, 0.3, 0.1, 0.03, 0.01, 0.003 and 0.001 μM). As shown in Fig. 3, the kinetic measurements indicated that the elicited inhibition increased by increasing the time; a characteristic of irreversible inhibition reaction considering the fact that interaction of irreversible inhibitors with the target protein involves an initial physical binding phase followed by a second phase of chemical interaction to set up a covalent bond. Following the published method for calculation of K_{inact} values [35], nonlinear regression, after calculating the K_{obs} for each concentration of compound **7m**, returned K_{inact} value of 0.01 (min^{-1}).

2.2.3. In silico docking simulation study

IKK-β consists of three domains: the kinase domain (K_D, residues 16–307), ubiquitin-like domain (ULD, residues 310–394), and scaffold dimerization domain (SDD, 410–666) 3QA8) [30]. The allosteric site allocated in the K_D of IKK-β incorporates a cysteine residue (Cys46) as a part of a short loop structure linking a short β-sheet structure (residues 41–44) with α-helix structure (residues 52–64). The kinase activity of IKK-β is sensitive to changes at this site; mutation of Lys44 which is the last residue in the sequence of the β-sheet, meanwhile, is one residue away from Cys46 results in kinase activity loss of IKK-β [36]. Also, literature reports proved that the natural product covalent allosteric IKK-β inhibitor binds to Cys46 at an allosteric site [26,27]. Previous

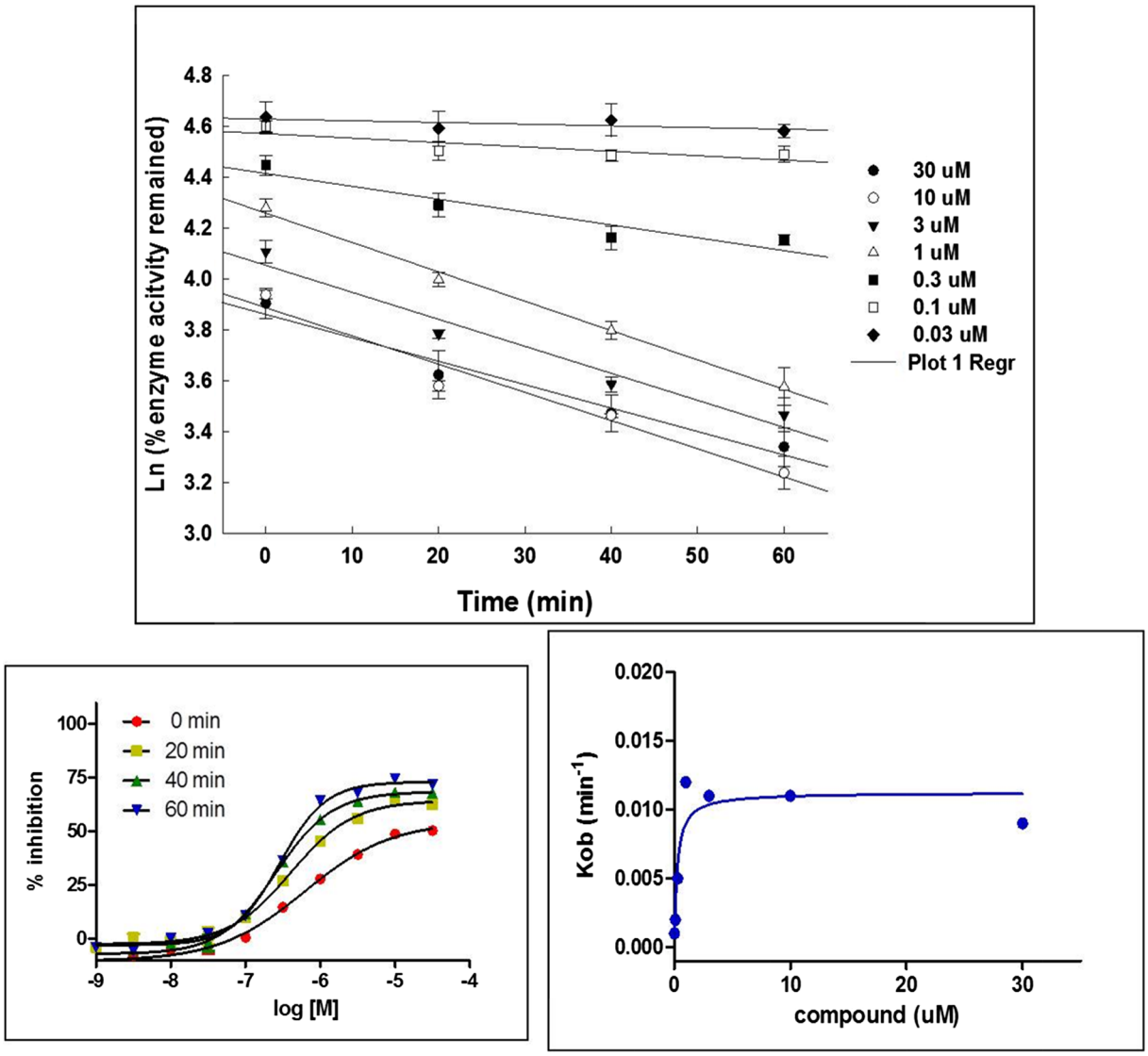

Fig. 3. Time-dependent dose-responses curves of compound **7m** and nonlinear regression of calculated K_{obs} values.

computational study showed that blocking solvent access to Trp58 is accompanied with inhibition of kinase activity evidenced by the finding that Trp58 is completely buried as in previous report of Ainsliadimer [26].

For better understanding of the molecular behaviors that triggered the elicited different inhibitory activities of the newly synthesized analogs over IKK-β, a molecular simulation study was conducted using the crystal structure of IKK-β (protein databank code: 3QA8). In this regard, covalent docking of a representative set including the inactive compound **7g**, the partially active compound **7i** and the most active compound **7m** has been carried out *via* CovDock workflow as implemented in Schrödinger Suite. In such protocol, a covalent docking of the ligand has been performed followed by energy minimization of Ligand-protein complex adduct. The top five poses were retrieved and analyzed visually. The top scoring pose of the most active compound **7m** showed the *N*-methylpiperazine moiety directed towards the α-helix where Trp58 is buried (Fig. 4). This binding mode is stabilized *via* favorable hydrophobic interactions with Tyr28, Arg47, Cys46, Arg55 and Leu91, in addition to hydrogen bonding interaction with Gln48. Also, the second best pose of compound **7m** presented similar binding mode which is stabilized by favorable hydrophobic interactions with Tyr28, Arg47 and Leu91, cation interaction with Arg55, as well as hydrogen bonding interactions with Gln48 and Arg55.

For the inactive analog **7g**; the best scoring calculated binding mode upon covalent docking showed lower score with a flipped interaction mode compared to the active compound **7m** (Fig. 5A). In this binding mode, the *N*-methylpiperazine moiety was directed away from the α-helix containing Trp58 while the imidazole ring at 3-position of the phenyl moiety is unable to block solvent access. Consequently, Trp58 might experience some solvent exposure which is, as mentioned previously, accompanying the activity of IKK-β. Despite this binding mode of compound **7g** lacks the favorable hydrophobic interactions with Tyr28 and Arg47, it is stabilized by a network of hydrophobic interactions with Trp32, Leu86, Pro88 and Leu91, as well as, hydrogen bonding interactions with Arg20, Gln48 and Arg55.

In comparison, both of the binding modes detected for the active and inactive compounds have been elicited by compound **7i** which exhibited a limited inhibition over IKK-β. The best scoring binding mode was the flipped binding mode in which the linked *N*-methylpiperazinyl-alkyl moiety was directed away from the α-helix (Fig. 5B). In this binding mode, the *N*-methylpiperazine which is directly attached to the benzylidene moiety is pointing towards the α-helix, however, it does not extend enough to block the access of solvent. Such binding mode is stabilized by hydrophobic interactions with Cys46, Leu86, Pro88, and Leu91, hydrogen bonding interactions with Gln45, Arg55 and Asp90, as well as, π-anion interaction with Glu49. As shown in

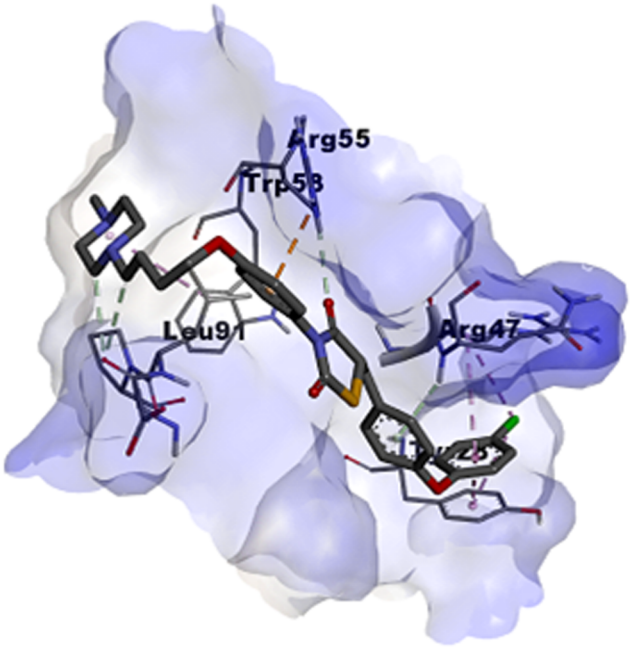

Fig. 4. The best scoring binding mode of covalently docked compound **7m**.

Fig. 5C, the second best calculated binding mode for compound **7i** was that in which the linked *N*-methylpiperazinyl-butyl moiety was directed towards the α-helix. This binding mode is stabilized by hydrophobic interactions with Cys46 and Leu91, hydrogen bonding interactions with Gln48, Gln49 and Arg55, in addition to, π-anion interaction with Glu49. In lieu of these mixed binding modes, the limited activity of compound **7i** would be understandable.

3. Experimental

3.1. Chemistry

General: All chemicals and reagents were purchased from commercial suppliers unless otherwise mentioned and used without further purification. The NMR spectra were obtained on Bruker Avance 400. ^{1}H NMR spectra were referenced to tetramethylsilane (δ = 0.00 ppm) as an internal standard. Column chromatography was performed on Merck Silica Gel 60 (230–400 mesh). TLC was carried out using glass sheets pre-coated with silica gel 60 F_{254} purchased by Merk. High-resolution spectra were performed on Waters ACQUITY UPLC BEH C18 1.7μ−Q-TOF SYNAPT G2-Si High Definition Mass Spectrometry. HRMS and HPLC purity charts, preparation of 4-(3,4,5-trifluorophenoxy)benzaldehyde reagent, NMR charts as well as LC and MS conditions have been added to this article in the supplementary file. Synthesis of intermediates **2**, **3**, **4**, and **5** has been reported in our recent publication [29].

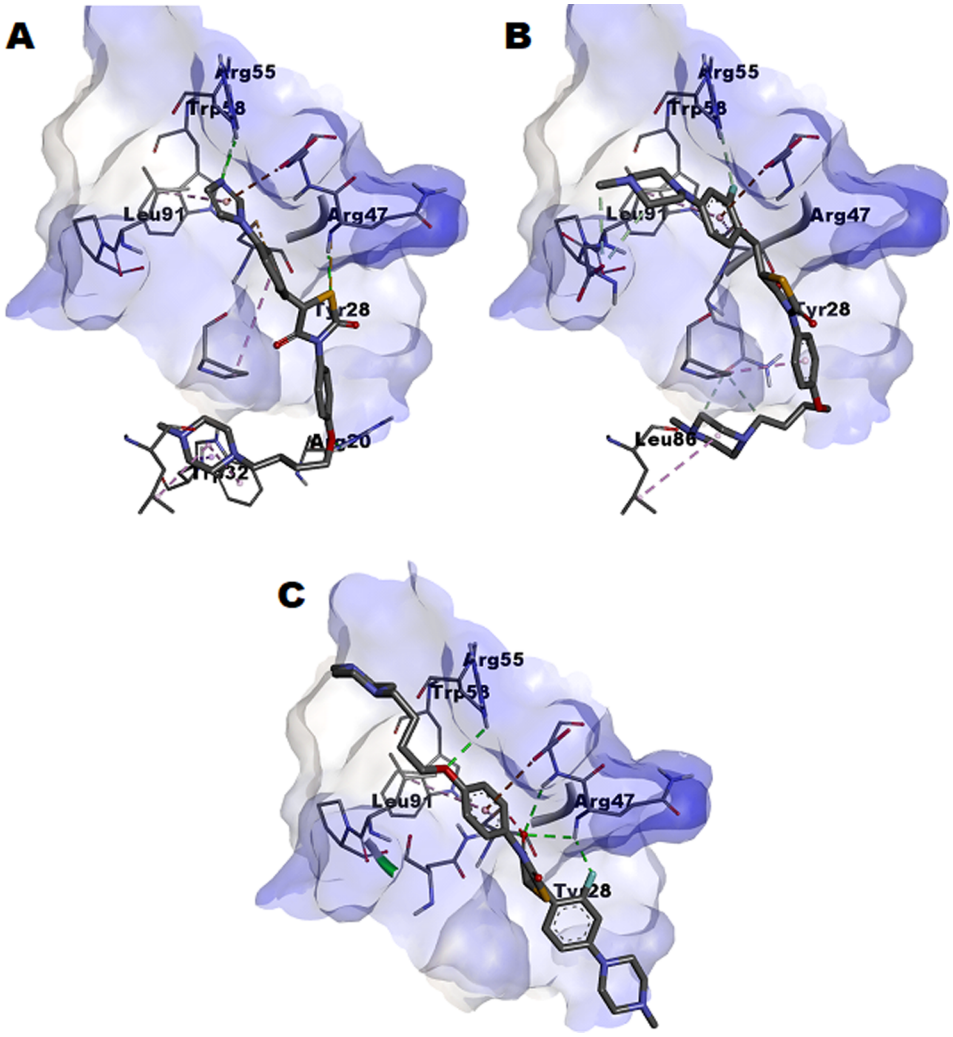

Fig. 5. The structures of covalently docked compound **7 g** and **7i**: A) The best scoring binding mode of compound **7g**; B) The best scoring binding mode of compound **7i**; C) The second best scoring binding mode of compound **7i**.

*3.1.1. Synthesis of 3-(4-(4-(4-methylpiperazin-1-yl)butoxy)phenyl) thiazolidine-2,4-dione (**6**)*

1-Methylpiperazine (0.15 mL, 1.34 mmol) was added to a solution of intermediate **5** (262.1 mg, 0.67 mmol) and potassium carbonate (180 mg, 1.34 mmol) in acetonitrile (3 mL). The reaction mixture was stirred at room temperature for 9 h. The mixture was quenched by addition of water and extracted with dichloromethane. The organic layer was dried over anhydrous $MgSO_4$, filtered and evaporated under reduced pressure. The residue was purified by column chromatography (SiO_2, DCM/MeOH 15:1 v/v including 1% of ammonium hydroxide) to yield the desired product **6**. White solid, yield: 57%, ^{1}H NMR (400 MHz, DMSO-d_6) δ 1.64–1.70 (m, 2H), 1.78–1.83 (m, 2H), 2.29 (s, 3H), 2.38–2.50 (m, 10H), 3.99 (t, J = 6.3 Hz, 2H), 4.09 (s, 2H), 6.97 (d, J = 8.9 Hz, 2H), 7.14 (d, J = 8.9 Hz, 2H). HRMS (ES+): m/z calculated for $C_{18}H_{25}N_3O_3S$: 364.1695 $[M+H]^+$. Found 364.1687.

*3.1.2. General procedure of target compounds (**7a–r**)*

NaOAc anhydrous (17.6 mg, 0.21 mmol), the appropriate aldehyde derivative (0.14 mmol), and intermediate **6** (25.4 mg, 0.07 mmol) were dissolved in AcOH (3 mL) and stirred at 110 °C for 16 h. After cooling, the mixture was neutralized to pH 8 by addition of NH_4OH and extracted with DCM. The organic layer was dried over anhydrous $MgSO_4$, filtered and concentrated under reduced pressure. The residue was purified by column chromatography (SiO_2, DCM/MeOH 15/1 v/v including 1% of NH_4OH) to produce the final target compounds.

*3.1.2.1. (Z)-5-((2,3-Dihydrobenzofuran-5-yl)methylene)-3-(4-(4-(4-methylpipera zin-1-yl)butoxy)phenyl)thiazolidine-2,4-dione (**7a**)*. Light brown solid, yield: 14%, HPLC purity: 4.48 min, 98.86%, ^{1}H NMR (400 MHz, $CDCl_3$) δ 1.65–1.70 (m, 2H), 1.79–1.84 (m, 2H), 2.31 (s, 3H), 2.38–2.59 (m, 10H), 3.29 (t, J = 8.7 Hz, 2H), 4.01 (t, J = 6.2 Hz, 2H), 4.67 (t, J = 8.7 Hz, 2H), 6.89 (d, J = 8.2 Hz, 1H), 7.00 (d, J = 8.9 Hz, 2H), 7.22 (d, J = 9.0 Hz, 2H), 7.35 (d, J = 8.4 Hz, 1H), 7.40 (s, 1H), 7.93 (s, 1H). ^{13}C NMR (100 MHz, $CDCl_3$) δ 14.10, 23.36, 27.17, 29.69, 45.89, 52.98, 55.00, 58.06, 68.00, 72.14, 110.32, 115.21, 117.20, 125.21, 126.08, 127.04, 128.49, 128.73, 132.32, 134.73, 159.44, 162.60, 166.21, 167.71. HRMS (ES+): m/z calculated for $C_{27}H_{31}N_3O_4S$: 494.2113 $[M+H]^+$. Found 494.2112.

*3.1.2.2. (Z)-3-(4-(4-(4-Methylpiperazin-1-yl)butoxy)phenyl)-5-((5-phenylthiophen-2-yl)methylene)thiazolidine-2,4-dione (**7b**)*. Yellow solid, yield: 13.6%, HPLC purity: 5.21 min, 98.28%, ^{1}H NMR (400 MHz, $CDCl_3$) δ 1.67–1.72 (m, 2H), 1.79–1.86 (m, 4H), 2.36 (s, 3H), 2.44–2.58 (m, 8H), 4.01 (t, J = 6.2 Hz, 2H), 6.99 (d, J = 8.9 Hz, 2H), 7.23 (d, J = 8.9 Hz, 2H), 7.37–7.46 (m, 5H), 7.67 (d, J = 8.6 Hz, 2H), 8.11 (s, 1H). HRMS (ES+): m/z calculated for $C_{29}H_{31}N_3O_3S_2$: 534.1885 $[M+H]^+$. Found 534.1888.

*3.1.2.3. (Z)-5-(4-(1H-Pyrazol-1-yl)benzylidene)-3-(4-(4-(4-methylpiperazin-1-yl)butoxy)phenyl)thiazolidine-2,4-dione (**7c**)*. Yellowish white solid, yield: 49%, ^{1}H NMR (400 MHz, DMSO-d_6) δ 1.29–1.38 (m, 2H), 1.60–1.62 (m, 2H), 1.74–1.78 (m, 2H), 2.24 (s, 3H), 2.38–2.44 (m, 8H), 4.06 (t, J = 6.5 Hz, 2H), 6.63 (s, 1H), 7.08 (d, J = 8.8 Hz, 2H), 7.36 (d, J = 8.5 Hz, 2H), 7.81–7.84 (m, 3H), 8.05 (d, J = 12.6 Hz, 2H), 8.08 (s, 1H), 8.64–8.65 (m, 1H). HRMS (ES^+): m/z calculated for $C_{28}H_{31}N_5O_3S$: 518.2226 $[M+H]^+$. Found 518.2233.

*3.1.2.4. (Z)-5-(4-(1H-1,2,4-triazol-1-yl)benzylidene)-3-(4-(4-(4-methylpiperazin-1-yl)butoxy)phenyl)thiazolidine-2,4-dione (**7d**)*. Yellowish white solid, yield: 32%, HPLC purity: 8.00 min, 92.60%, ^{1}H NMR (400 MHz, DMSO-d_6) δ 1.57–1.60 (m, 2H), 1.74–1.77 (m, 2H), 2.18 (s, 3H), 2.26–2.47 (m, 10H), 4.05 (t, J = 6.3 Hz, 2H), 7.08 (d, J = 8.6 Hz, 2H), 7.36 (d, J = 8.7 Hz, 2H), 7.88 (d, J = 8.5 Hz, 2H), 8.04 (s, 1H), 8.08 (d, J = 8.5 Hz, 2H), 8.32 (s, 1H), 9.43 (s, 1H). ^{13}C NMR (100 MHz, DMSO-d_6) δ 23.13, 26.93, 46.04, 52.94, 55.09, 57.69, 68.12, 115.33, 120.37, 122.63, 125.78, 129.70, 132.01, 132.13, 132.77, 138.03, 143.22, 153.27, 159.46, 165.80, 167.38. HRMS (ES+): m/z calculated for $C_{27}H_{30}N_6O_3S$: 519.2178 $[M+H]^+$. Found 519.2172.

*3.1.2.5. (Z)-5-(3-Chloro-4-(1H-pyrazol-1-yl)benzylidene)-3-(4-(4-(4-methylpiperazin-1-yl)butoxy)phenyl)thiazolidine-2,4-dione (**7e**)*. White solid, yield: 67%, HPLC purity: 8.40 min, 100%, ^{1}H NMR (400 MHz, DMSO-d_6) δ 1.54–1.61 (m, 2H), 1.71–1.78 (m, 2H), 2.14 (s, 3H), 2.30–2.33 (m, 10H), 4.04 (t, J = 6.4 Hz, 2H), 6.59 (t, J = 2.0 Hz, 1H), 7.07 (d, J = 9.0 Hz, 2H), 7.35 (d, J = 9.0 Hz, 2H), 7.75–7.83 (m, 3H), 8.03 (d, J = 1.8 Hz, 1H), 8.05 (s, 1H), 8.27 (d, J = 2.5 Hz, 1H). ^{13}C NMR (100 MHz, $CDCl_3$) δ 23.42, 27.18, 46.03, 53.16, 55.14, 58.13, 68.07, 107.41, 115.31, 123.58, 124.76, 127.92, 128.07, 128.38, 128.96, 131.23, 131.29, 132.33, 133.67, 139.08, 141.65, 159.65, 165.49, 166.66. HRMS (ES+): m/z calculated for $C_{28}H_{30}ClN_5O_3S$: 552.1836 $[M+H]^+$. Found 552.1833.

*3.1.2.6. (Z)-5-(3-Chloro-4-(1H-imidazol-1-yl)benzylidene)-3-(4-(4-(4-methylpiperazin-1-yl)butoxy)phenyl)thiazolidine-2,4-dione (**7f**)*. Yellow solid, yield: 58%, ^{1}H NMR (400 MHz, DMSO-d_6) δ 1.60–1.64 (m, 2H), 1.71–1.78 (m, 2H), 2.4 (s, 3H), 2.66–2.77 (m, 10H), 4.06 (t, J = 6.2 Hz, 2H), 7.09 (d, J = 8.9 Hz, 2H), 7.16 (s, 1H), 7.37 (d, J = 8.9 Hz, 2H), 7.55 (s, 1H), 7.76–7.77 (m, 2H), 8.02 (s, 1H), 8.05–8.06 (m, 2H). ^{13}C NMR (100 MHz, $CDCl_3$) δ 22.75, 26.75, 44.73, 51.64, 53.95, 57.05, 68.01, 115.05, 115.37, 121.30, 124.79, 125.74, 129.19, 129.32, 129.52, 129.63, 129.71, 130.58, 132.80, 135.13, 136.14, 138.21, 159.48, 165.61, 167.08. HRMS (ES+): m/z calculated for $C_{28}H_{30}ClN_5O_3S$: 552.1836 $[M+H]^+$. Found 552.1846.

*3.1.2.7. (Z)-5-(3-(1H-Imidazol-1-yl)benzylidene)-3-(4-(4-(4-methylpiperazin-1-yl)butoxy)phenyl)thiazolidine-2,4-dione (**7g**)*. Yellowish white solid, yield: 35%, HPLC purity: 3.33 min, 100%, ^{1}H NMR (400 MHz, DMSO-d_6) δ 1.57–1.60 (m, 2H), 1.74–1.77 (m, 2H), 2.18 (s, 3H), 2.32–2.37 (m, 10H), 4.05 (t, J = 5.9 Hz, 2H), 7.08 (d, J = 8.6 Hz, 2H), 7.17 (s, 1H), 7.36 (d, J = 8.6 Hz, 2H), 7.61 (d, J = 7.7 Hz, 1H), 7.73 (t, J = 7.9 Hz, 1H), 7.82–7.84 (m, 2H), 8.04 (s, 2H), 8.36 (s, 1H). ^{13}C NMR (100 MHz, DMSO-d_6) δ 23.13, 26.93, 46.04, 52.94, 55.10, 57.68, 68.12, 115.34, 118.38, 122.41, 123.15, 123.67, 125.74, 127.06, 129.70, 130.66, 131.46, 132.14, 135.24, 136.05, 138.09, 159.48, 165.77, 167.34. HRMS (ES^+): m/z calculated for $C_{28}H_{31}N_5O_3S$: 518.2226 $[M+H]^+$. Found 518.2228.

*3.1.2.8. (Z)-5-(3-Chloro-4-morpholinobenzylidene)-3-(4-(4-(4-methylpiperazin-1-yl)butoxy)phenyl)thiazolidine-2,4-dione (**7h**)*. Yellow solid, yield: 28%, HPLC purity: 8.45 min, 91.45%, ^{1}H NMR (400 MHz, $CDCl_3$) δ 1.67–1.73 (m, 2H), 1.83–1.88 (m, 2H), 1.99 (bs, 2H), 2.36 (s, 3H), 2.45–2.57 (m, 8H), 3.2 (t, J = 4.5 Hz, 4H), 3.92 (t, J = 4.4 Hz, 4H), 4.04 (t, J = 6.2 Hz, 2H), 7.02 (d, J = 8.9 Hz, 2H), 7.13 (d, J = 8.4 Hz, 1H), 7.25 (d, J = 8.9 Hz, 2H), 7.46 (dd, J = 2.1, 8.4 Hz, 1H), 7.58 (d, J = 2.1 Hz, 1H), 7.88 (s, 1H). ^{13}C NMR (100 MHz, $CDCl_3$) δ 23.30, 27.13, 45.75, 51.20, 52.80, 54.85, 57.99, 66.90, 67.98, 115.25, 120.16, 120.40, 124.98, 128.44, 128.54, 128.78, 129.70, 132.58, 132.83, 150.81, 159.51, 165.84, 167.22. HRMS (ES+): m/z calculated for $C_{29}H_{35}ClN_4O_4S$: 571.2146 $[M+H]^+$. Found 571.2197.

*3.1.2.9. (Z)-5-(2-Fluoro-4-(4-methylpiperazin-1-yl)benzylidene)-3-(4-(4-(4-methylpiperazin-1-yl)butoxy)phenyl)thiazolidine-2,4-dione (**7i**)*. Brown solid, yield: 31%, HPLC purity: 3.40 min, 100%, ^{1}H NMR (400 MHz, $CDCl_3$) δ 1.66–1.71 (m, 2H), 1.78–1.83 (m, 2H), 2.05 (bs, 4H), 2.32 (s, 3H), 2.35 (s, 3H), 2.43 (t, J = 7.5 Hz, 2H), 2.49–2.59 (m, 8H), 3.37 (t, J = 5.0 Hz, 4H), 4.00 (t, J = 6.1 Hz, 2H), 6.57–6.61 (dd, J = 2.4, 14.0 Hz, 1H), 6.72–6.75 (dd, J = 2.24, 8.96 Hz, 1H), 6.98 (d, J = 8.8 Hz, 2H), 7.22 (d, J = 8.9 Hz, 2H), 7.41 (t, J = 8.8 Hz, 1H), 8.12 (s, 1H). ^{13}C NMR (100 MHz, $CDCl_3$) δ 23.29, 27.13, 45.73, 46.06, 47.07, 52.77, 54.52, 54.84, 57.99, 67.99, 101.05, 110.27, 115.19, 125.28, 126.74, 128.51, 130.09, 159.38. HRMS (ES+): m/z calculated

for $C_{30}H_{38}FN_5O_3S$: 568.2757 $[M+H]^+$. Found 568.2759.

*3.1.2.10. (Z)-3-(4-(4-(4-Methylpiperazin-1-yl)butoxy)phenyl)-5-(3-morpholinobenzylidene)thiazolidine-2,4-dione (**7j**)*. Yellow solid, yield: 24%, HPLC purity: 4.43 min, 100%, ^{1}H NMR (400 MHz, $CDCl_3$) δ 1.66–1.70 (m, 2H), 1.80–1.84 (m, 2H), 2.33 (s, 3H), 2.39–2.60 (m, 10H), 3.21 (t, J = 4.5 Hz, 4H), 3.89 (t, J = 6.1 Hz, 4H), 4.01 (t, J = 6.2 Hz, 2H), 6.98–7.06 (m, 5H), 7.22 (d, J = 8.9 Hz, 2H), 7.39 (t, J = 8.7 Hz, 1H), 7.94 (s, 1H). ^{13}C NMR (100 MHz, $CDCl_3$) δ 23.27, 27.12, 45.71, 48.90, 52.72, 54.81, 57.96, 66.76, 67.97, 115.25, 116.72, 117.88, 121.01, 121.68, 124.99, 128.46, 130.04, 134.20, 134.98, 151.80, 159.49, 165.91, 167.60. HRMS (ES+): *m/z* calculated for $C_{29}H_{36}N_4O_4S$: 537.2535 $[M+H]^+$. Found 537.2529.

*3.1.2.11. (Z)-3-(4-(4-(4-Methylpiperazin-1-yl)butoxy)phenyl)-5-(4-(4-nitrophenoxy)benzylidene)thiazolidine-2,4-dione (**7k**)*. Yellow solid, yield: 38%, ^{1}H NMR (400 MHz, $CDCl_3$) δ 1.66–1.69 (m, 2H), 1.81–1.84 (m, 2H), 2.29 (s, 3H), 2.39–2.43 (m, 10H), 4.01 (t, J = 6.2 Hz, 2H), 7.01 (d, J = 8.9 Hz, 2H), 7.13 (d, J = 8.7 Hz, 2H), 7.18–7.25 (m, 4H), 7.60 (d, J = 8.7 Hz, 2H), 7.97 (s, 1H), 8.27 (d, J = 9.1 Hz, 2H). HRMS (ES+): *m/z* calculated for $C_{31}H_{32}N_4O_6S$: 589.2121 $[M+H]^+$. Found 589.2134.

*3.1.2.12. (Z)-4-(4-((3-(4-(4-(4-Methylpiperazin-1-yl)butoxy)phenyl)-2,4-dioxothiazolidin-5-ylidene)methyl)phenoxy)benzonitrile (**7l**)*. Light brown solid, yield: 33%, HPLC purity: 5.23 min, 98.00%, ^{1}H NMR (400 MHz, $CDCl_3$) δ 1.64–1.71 (m, 2H), 1.79–1.86 (m, 4H), 2.30 (s, 3H), 2.39–2.59 (m, 8H), 4.01 (t, J = 6.2 Hz, 2H), 7.00 (d, J = 8.8 Hz, 2H), 7.11 (d, J = 8.7 Hz, 2H), 7.16 (d, J = 8.6 Hz, 2H), 7.23 (d, J = 8.8 Hz, 2H), 7.59 (d, J = 8.6 Hz, 2H), 7.67 (d, J = 8.6 Hz, 2H) 7.96 (s, 1H). ^{13}C NMR (100 MHz, $CDCl_3$) δ 23.40, 27.18, 45.98, 53.10, 55.09, 58.11, 68.04, 107.32, 115.27, 119.18, 120.23, 120.78, 124.90, 128.43, 129.74, 132.37, 133.01, 134.38, 157.14, 159.58, 160.11, 165.87, 167.20.

*3.1.2.13. (Z)-5-(4-(4-Chlorophenoxy)benzylidene)-3-(4-(4-(4-methylpiperazin-1-yl)butoxy)phenyl)thiazolidine-2,4-dione (**7m**)*. White solid, yield: 52%, ^{1}H NMR (400 MHz, $CDCl_3$) δ 1.64–1.71 (m, 2H), 1.79–1.86 (m, 4H), 2.29 (s, 3H), 2.39–2.49 (m, 8H), 4.01 (t, J = 6.3 Hz, 2H), 6.98–7.07 (m, 6H), 7.22 (d, J = 9.0 Hz, 2H), 7.36 (d, J = 8.9 Hz, 2H), 7.52 (d, J = 8.8 Hz, 2H), 7.94 (s, 1H). ^{13}C NMR (100 MHz, $CDCl_3$) δ 23.41, 27.19, 46.02, 53.15, 55.12, 58.13, 68.03, 115.25, 118.45, 119.67, 121.34, 125.00, 128.16, 128.45, 129.79, 130.12, 132.28, 133.52, 154.20, 159.53, 165.98, 167.42. HRMS (ES+): *m/z* calculated for $C_{31}H_{32}ClN_3O_4S$: 578.1880 $[M+H]^+$. Found 578.1893.

*3.1.2.14. (Z)-5-(4-(2,4-Dichlorophenoxy)benzylidene)-3-(4-(4-(4-methylpiperazin-1-yl)butoxy)phenyl)thiazolidine-2,4-dione (**7n**)*. White solid, yield: 37%, HPLC purity: 9.08 min, 95.08%, ^{1}H NMR (400 MHz, $CDCl_3$) δ 1.64–1.71 (m, 2H), 1.75 (bs, 2H), 1.79–1.85 (m, 2H), 2.30 (s, 3H), 2.40–2.48 (m, 8H), 4.01 (t, J = 6.2 Hz, 2H), 6.98–7.02 (m, 4H), 7.06 (d, J = 8.6 Hz, 1H), 7.22 (d, J = 8.8 Hz, 2H), 7.28 (dd, J = 2.4, 8.6 Hz, 1H), 7.51 (s, 1H), 7.53 (d, J = 6.6 Hz, 2H), 7.93 (s, 1H). ^{13}C NMR (100 MHz, $CDCl_3$) δ 23.40, 27.18, 45.98, 53.10, 55.09, 58.11, 68.02, 115.25, 117.49, 119.79, 123.12, 124.99, 127.71, 128.31, 128.45, 128.47, 130.84, 132.30, 133.42, 149.70, 158.88, 159.53, 165.96, 167.39. HRMS (ES+): *m/z* calculated for $C_{31}H_{31}Cl_2N_3O_4S$: 612.1490 $[M+H]^+$. Found 612.1494.

*3.1.2.15. (Z)-5-(4-(2,4-Difluorophenoxy)benzylidene)-3-(4-(4-(4-methylpiperazin-1-yl)butoxy)phenyl)thiazolidine-2,4-dione (**7o**)*. Yellowish white solid, yield: 46%, ^{1}H NMR (400 MHz, $CDCl_3$) δ 1.68–1.72 (m, 2H), 1.80–1.84 (m, 2H), 2.01–2.04 (m, 2H), 2.34 (s, 3H), 2.43–2.55 (m, 8H), 4.01 (t, J = 6.4 Hz, 2H), 6.80–6.83 (m, 1H), 6.90–6.95 (m, 1H), 7.00 (d, J = 8.7 Hz, 2H), 7.07 (d, J = 8.5 Hz, 2H), 7.15–7.23 (m, 3H), 7.53 (d, J = 8.6 Hz, 2H), 7.94 (s, 1H). ^{13}C NMR (100 MHz, $CDCl_3$) δ 23.25, 27.12, 45.64, 52.66, 54.75, 67.96, 109.65, 109.84, 115.26, 115.68, 118.49, 128.46, 132.31, 133.38, 159.13, 159.51, 165.95, 167.37. HRMS (ES+): *m/z* calculated for $C_{31}H_{31}F_2N_3O_4S$: 580.2081 $[M+H]^+$. Found 580.2076.

*3.1.2.16. (Z)-5-(4-(3,4-Difluorophenoxy)benzylidene)-3-(4-(4-(4-methylpiperazin-1-yl)butoxy)phenyl)thiazolidine-2,4-dione (**7p**)*. White solid, yield: 58%, HPLC purity: 8.78 min, 98.18%, ^{1}H NMR (400 MHz, $CDCl_3$) δ 1.65–1.71 (m, 2H), 1.79–1.84 (m, 2H), 2.29 (s, 3H), 2.39–2.48 (m, 10H), 4.01 (t, J = 6.2 Hz, 2H), 6.80–6.84 (m, 1H), 6.90–6.95 (m, 1H), 7.00 (d, J = 8.9 Hz, 2H), 7.07 (d, J = 8.7 Hz, 2H), 7.15–7.23 (m, 3H), 7.53 (d, J = 8.7 Hz, 2H), 7.93 (s, 1H). HRMS (ES+): *m/z* calculated for $C_{31}H_{31}F_2N_3O_4S$: 580.2081 $[M+H]^+$. Found 580.2075.

*3.1.2.17. (Z)-3-(4-(4-(4-Methylpiperazin-1-yl)butoxy)phenyl)-5-(4-(3,4,5-trifluorophenoxy)benzylidene)thiazolidine-2,4-dione (**7q**)*. Yellowish white solid, yield: 40%, HPLC purity: 8.90 min, 97.63%, ^{1}H NMR (400 MHz, $CDCl_3$) δ 1.66–1.69 (m, 2H), 1.80–1.84 (m, 2H), 2.3 (s, 3H), 2.41–2.51 (m, 10H), 4.01 (t, J = 6.4 Hz, 2H), 6.71 (t, J = 6.7 Hz, 2H), 7.00 (d, J = 8.8 Hz, 2H), 7.10 (d, J = 8.8 Hz, 2H), 7.22 (d, J = 9.2 Hz, 2H), 7.56 (d, J = 8.4 Hz, 2H), 7.94 (s, 1H). ^{13}C NMR (100 MHz, $CDCl_3$) δ 23.36, 27.16, 45.90, 53.00, 55.00, 58.07, 68.01, 104.13, 104.37, 115.25, 119.26, 120.54, 124.94, 128.43, 129.29, 132.35, 133.06, 157.92, 159.54, 165.87, 167.23. HRMS (ES+): *m/z* calculated for $C_{31}H_{30}F_3N_3O_4S$: 598.1987 $[M+H]^+$. Found 598.1992.

*3.1.2.18. (Z)-4-(4-((3-(4-(4-(4-Methylpiperazin-1-yl)butoxy)phenyl)-2,4-dioxothiazolidin-5-ylidene)methyl)phenoxy)phthalonitrile (**7r**)*. White solid, yield: 24%, HPLC purity: 8.62 min, 92.16%, ^{1}H NMR (400 MHz, $CDCl_3$) δ 1.66–1.72 (m, 2H), 1.79–1.86 (m, 2H), 2.29 (s, 3H), 2.40–2.48 (m, 10H), 4.02 (t, J = 6.4 Hz, 2H), 7.01 (d, J = 9.2 Hz, 2H), 7.20 (d, J = 8.8 Hz, 2H), 7.23 (d, J = 8.8 Hz, 2H), 7.32 (dd, J = 2.4, 8.8 Hz, 1H), 7.37 (d, J = 2.4 Hz, 1H), 7.65 (d, J = 8.8 Hz, 2H), 7.78 (d, J = 8.8 Hz, 1H), 7.97 (s, 1H). ^{13}C NMR (100 MHz, $CDCl_3$) δ 23.41, 27.19, 46.00, 53.12, 55.11, 58.12, 68.07, 110.06, 114.69, 115.09, 115.30, 118.01, 120.95, 121.88, 122.21, 122.38, 124.83, 128.41, 131.17, 132.40, 132.59, 135.61, 155.38, 159.63, 160.56, 165.73, 166.94. HRMS (ES+): *m/z* calculated for $C_{33}H_{31}N_5O_4S$: 594.2175 $[M+H]^+$. Found 594.2176.

3.2. Biological evaluation

3.2.1. In vitro IMAP® TR-FRET assay of IKK-β

It was conducted as reported in our recent publication [29] and included in the supplementary materials.

3.2.2. Molecular modeling study

The ligands was sketched, energy minimized and prepared using tools of Schrödinger's Maestro. The crystal structure of IKK-β was retrieved from protein databank (PDB code: 3QA8). The structure was prepared using the protein preparation wizard implemented in Schrödinger. Chain A was used for performing the covalent docking study. The covalent docking procedure was performed according to covalent docking protocol without any constraint and defining Cys46 as the reactive residue in a Michael-type addition reaction. Affinity scores were calculated using Glide and the best scoring five poses were retrieved, and analyzed.

4. Conclusion

As a conclusion, a new series of thiazolidine-2,4-dione analogs with promising IKK-β inhibitory activity was acquired *via* an optimization strategy approach. Successfully, higher level of potency was obtained, as aimed, and the Structure-Activity-Relationship (SAR) well-explained the differences of the elicited biological activities. Also, the mechanistic and docking simulation studies, performed for the most active analog

7m, presented a promising investigational candidate worthy of further evaluation towards a novel therapy for IKK- β related diseases.

Declaration of Competing Interest

Authors have declared no conflict of interest.

Acknowledgement

This work was supported by the KIST Institutional programs (Grant No. 2E29260) from Korea Institute of Science and Technology and by the Creative Fusion Research Program through the Creative Allied Project funded by the National Research Council of Science & Technology (CAP-12-1-KIST).

Appendix A. Supplementary material

Supplementary data to this article can be found online at https://doi.org/10.1016/j.bioorg.2019.103261.

References

[1] D. Huang, T. Zhou, K. Lafleur, C. Nevado, A. Caflisch, Kinase selectivity potential for inhibitors targeting the ATP binding site: a network analysis, Bioinformatics 26 (2010) 198–204.
[2] Z. Fang, C. Grutter, D. Rauh, Strategies for the selective regulation of kinases with allosteric modulators: exploiting exclusive structural features, ACS Chem. Biol. 8 (2013) 58–70.
[3] S. Muller, S. Knapp, CHAPTER 3 Targeting Catalytic and Non-Catalytic Functions of Protein Kinases, in: Allosterism in Drug Discovery, The Royal Society of Chemistry, 2017, pp. 40-64.
[4] A.H.E. Hassan, H.R. Park, Y.M. Yoon, H.I. Kim, S.Y. Yoo, K.W. Lee, Y.S. Lee, Antiproliferative 3-deoxysphingomyelin analogs: Design, synthesis, biological evaluation and molecular docking of pyrrolidine-based 3-deoxysphingomyelin analogs as anticancer agents, Bioorg. Chem. 84 (2019) 444–455.
[5] S. De Cesco, J. Kurian, C. Dufresne, A.K. Mittermaier, N. Moitessier, Covalent inhibitors design and discovery, Eur. J. Med. Chem. 138 (2017) 96–114.
[6] A.M. Gilbert, Recent advances in irreversible kinase inhibitors, Pharm. Pat. Anal. 3 (2014) 375–386.
[7] Q. Liu, Y. Sabnis, Z. Zhao, T. Zhang, S.J. Buhrlage, L.H. Jones, N.S. Gray, Developing irreversible inhibitors of the protein kinase cysteinome, Chem. Biol. 20 (2013) 146–159.
[8] C. González-Bello, Designing Irreversible Inhibitors—Worth the Effort? ChemMedChem 11 (2016) 22–30.
[9] K. Sanderson, Irreversible kinase inhibitors gain traction, Nat. Rev. Drug Discov. 12 (2013) 649–651.
[10] L. Garuti, M. Roberti, G. Bottegoni, Irreversible protein kinase inhibitors, Curr. Med. Chem. 18 (2011) 2981–2994.
[11] Z. Zhao, P.E. Bourne, Progress with covalent small-molecule kinase inhibitors, Drug Discov. Today 23 (2018) 727–735.
[12] S. Lu, J. Zhang, Designed covalent allosteric modulators: an emerging paradigm in drug discovery, Drug Discov. Today 22 (2017) 447–453.
[13] J. Weisner, R. Gontla, L. van der Westhuizen, S. Oeck, J. Ketzer, P. Janning, A. Richters, T. Mühlenberg, Z. Fang, A. Taher, V. Jendrossek, S.C. Pelly, S. Bauer, W.A.L. van Otterlo, D. Rauh, Covalent-Allosteric Kinase Inhibitors, Angew. Chem., Int. Ed. 54 (2015) 10313–10316.
[14] T. Liu, L. Zhang, D. Joo, S.-C. Sun, NF-κB signaling in inflammation, Signal Transduct. Target. Ther. 2 (2017) 17023, https://doi.org/10.1038/sigtrans.2017.23.
[15] D.S. Straus, Design of small molecules targeting transcriptional activation by NF-κB: overview of recent advances, Expert Opin. Drug Discov. 4 (2009) 823–836.
[16] S.C. Gupta, C. Sundaram, S. Reuter, B.B. Aggarwal, Inhibiting NF-κB activation by small molecules as a therapeutic strategy, Biochim. Biophys. Acta, Gene Regul. Mech. 1799 (2010) 775–787.
[17] A.H.E. Hassan, S.Y. Yoo, K.W. Lee, Y.M. Yoon, H.W. Ryu, Y. Jeong, J.S. Shin, S.Y. Kang, S.Y. Kim, H.H. Lee, B.Y. Park, K.T. Lee, Y.S. Lee, Repurposing moslo-flavone/5,6,7-trimethoxyflavone-resveratrol hybrids: Discovery of novel p38-alpha MAPK inhibitors as potent interceptors of macrophage-dependent production of proinflammatory mediators, Eur. J. Med. Chem. 180 (2019) 253–267.
[18] T.D. Gilmore, M. Herscovitch, Inhibitors of NF-kappaB signaling: 785 and counting, Oncogene 25 (2006) 6887–6899.
[19] A.H.E. Hassan, E. Choi, Y.M. Yoon, K.W. Lee, S.Y. Yoo, M.C. Cho, J.S. Yang, H.I. Kim, J.Y. Hong, J.S. Shin, K.S. Chung, J.H. Lee, K.T. Lee, Y.S. Lee, Natural products hybrids: 3,5,4'-Trimethoxystilbene-5,6,7-trimethoxyflavone chimeric analogs as potential cytotoxic agents against diverse human cancer cells, Eur. J. Med. Chem. 161 (2019) 559–580.
[20] J.A. Schmid, A. Birbach, IkappaB kinase beta (IKKbeta/IKK2/IKBKB)–a key molecule in signaling to the transcription factor NF-kappaB, Cytokine Growth Factor Rev. 19 (2008) 157–165.
[21] M. Karin, Y. Yamamoto, Q.M. Wang, The IKK NF-kappa B system: a treasure trove for drug development, Nat. Rev. Drug Discov. 3 (2004) 17–26.
[22] J.K. Durand, A.S. Baldwin, Targeting IKK and NF-κB for Therapy, Adv. Protein Chem. Struct. Biol. 107 (2017) 77–115.
[23] C. Gamble, K. McIntosh, R. Scott, K.H. Ho, R. Plevin, A. Paul, Inhibitory kappa B kinases as targets for pharmacological regulation, Br. J. Pharmacol. 165 (2012) 802–819.
[24] A. Elkamhawy, A.H.E. Hassan, S. Paik, Y. Sup Lee, H.H. Lee, J.S. Shin, K.T. Lee, E.J. Roh, EGFR inhibitors from cancer to inflammation: Discovery of 4-fluoro-N-(4-(3-(trifluoromethyl)phenoxy)pyrimidin-5-yl)benzamide as a novel anti-inflammatory EGFR inhibitor, Bioorg. Chem. 86 (2019) 112–118.
[25] J.J. Huang, H.X. Chu, Z.Y. Jiang, X.J. Zhang, H.P. Sun, Q.D. You, Recent advances in the structure-based and ligand-based design of IKKbeta inhibitors as anti-inflammation and anti-cancer agents, Curr. Med. Chem. 21 (2014) 3893–3917.
[26] T. Dong, C. Li, X. Wang, L. Dian, X. Zhang, L. Li, S. Chen, R. Cao, L. Li, N. Huang, S. He, X. Lei, Ainsliadimer A selectively inhibits IKKα/β by covalently binding a conserved cysteine, Nat. Commun. 6 (2015) 6522.
[27] F. Yan, F. Yang, R. Wang, X.J. Yao, L. Bai, X. Zeng, J. Huang, V.K.W. Wong, C.W.K. Lam, H. Zhou, X. Su, J. Liu, T. Li, L. Liu, Isoliquiritigenin suppresses human T Lymphocyte activation via covalently binding cysteine 46 of IκB kinase, Oncotarget 8 (2017) 34223–34235.
[28] H. Park, Y. Shin, H. Choe, S. Hong, Computational Design and Discovery of Nanomolar Inhibitors of IκB Kinase β, J. Am. Chem. Soc. 137 (2015) 337–348.
[29] A. Elkamhawy, N.Y. Kim, A.H.E. Hassan, J.E. Park, J.E. Yang, K.S. Oh, B.H. Lee, M.Y. Lee, K.J. Shin, K.T. Lee, W. Hur, E.J. Roh, Design, synthesis and biological evaluation of novel thiazolidinedione derivatives as irreversible allosteric IKK-beta modulators, Eur. J. Med. Chem. 157 (2018) 691–704.
[30] G. Xu, Y.-C. Lo, Q. Li, G. Napolitano, X. Wu, X. Jiang, M. Dreano, M. Karin, H. Wu, Crystal structure of inhibitor of κB kinase β (IKKβ), Nature 472 (2011) 325–330.
[31] S. Saxena, G. Samala, J.P. Sridevi, P.B. Devi, P. Yogeeswari, D. Sriram, Design and development of novel Mycobacterium tuberculosis L-alanine dehydrogenase inhibitors, Eur. J. Med. Chem. 92 (2015) 401–414.
[32] I.B. Levshin, I.V. Grigor'eva, A.A. Tsurkan, K.A. V'Yunov, A.I. Ginak, Study of azolidine reactivity and tautomerism. 53. Synthesis of 5-arylidene-2-(allylamino)-Δ2-thiazolin-4-ones and 5-arylidene-2-imino-3-allylthiazolidin-4-ones, Khim. Geterotsikl. Soedin. (1985) 494–497.
[33] S.Q. Tang, Y.Y.I. Lee, D.S. Packiaraj, H.K. Ho, C.L.L. Chai, Systematic Evaluation of the Metabolism and Toxicity of Thiazolidinone and Imidazolidinone Heterocycles, Chem. Res. Toxicol. 28 (2015) 2019–2033.
[34] J. Yong, M.Q. Christopher, K. Silvia, V.T. Robert, Current in vitro kinase assay technologies: the quest for a universal format, Curr. Drug Discov. Technol. 5 (2008) 59–69.
[35] R.S. Obach, R.L. Walsky, K. Venkatakrishnan, Mechanism-based inactivation of human cytochrome p450 enzymes and the prediction of drug-drug interactions, Drug Metab. Dispos. 35 (2007) 246–255.
[36] J.D. Woronicz, X. Gao, Z. Cao, M. Rothe, D.V. Goeddel, IκB Kinase-β: NF-κB activation and complex formation with IκB kinase-α and NIK, Science 278 (1997) 866–869.